Journal of Applied Polymer Science

Synthesis and Thermal Stability Properties of Boron-Doped Silicone Resin

Zhifeng Hao, Jin Zhang, Yahong Wu, Jian Yu, Lin Yu
School of Chemical Engineering and Light Industry, Guangdong University of Technology, Guangzhou 510006, People's Republic of China
Correspondence to: Z. F. Hao (E-mail: haozhifeng3377@163.com)

ABSTRACT: In this article, a novel boron-doped silicone resin (BSR) was synthesized by hydrolysis-polycondensation method, with propyl-triethoxysilane (PTES), dimethyl-diethoxysilane (DMDES), and boric acid (BA) as starting materials, using absolute ethyl alcohol as solvent and hydrochloric acid as catalyst. The structures of the BSR were characterized by Fourier transform infrared spectroscopy (FTIR), nuclear magnetic resonance (NMR), X-ray photoelectron spectroscopy (XPS), and gel permeation chromatography (GPC). FTIR spectra showed characteristic B—O—Si and Si—O—Si stretching modes. XPS and NMR results confirmed further that boron element was doped successfully into the main chains of the silicone resin as Si—O—B bond motifs, and hydroxyl groups from BA were condensed properly with Si—OH or Si—OR to form cross-linked structure of BSR with narrowed molecular weight distributions in optimum experimental condition. The thermal stability of the BSR was studied by thermogravimetry analysis and derivative thermogravimetry. The thermal degradation temperature of the silicone resin improved greatly after doping element boron into the main chain, and the thermal stability of the BSR was influenced by the content of boron. The thermal degradation mechanism of this BSR was also discussed. The degradation process can be divided into two stages, the weight loss in the first stages may be corresponding to the loss of the small groups and weaker bonds in the chains, such as $-CH_3$, and $-C_3H_7$, the weight loss in the second stage may be corresponding to the loss of the group as $-OC_2H_5$. © 2014 Wiley Periodicals, Inc. J. Appl. Polym. Sci. **2014**, *131*, 40934.

KEYWORDS: degradation; polycondensation; resins; thermal properties; thermogravimetric analysis (TGA)

Received 12 August 2013; accepted 26 April 2014
DOI: 10.1002/app.40934

INTRODUCTION

Silicone resins with excellent thermal resistance have been applied broadly in industry, due to the high energy of Si—O bond (451 kJ/mol) on the main chain. Varnishes based on silicone resins with phenyl groups on the branched-chain have a thermal stability from 200 to 250°C. With flexible Si—O—Si bond angle (from 140° to 180°) and long Si—O bond length (1.64 Å), it is relatively easy to do some modifications on the chain of silicone resins. In order to improve thermal resistant properties of silicone resins, one method used commonly is to dope these resins with B, Ti, Al, Sn, Pb, and other inorganic elements into the silicone backbone (—Si—O—),[1–6] leading to an increased thermal resistance. Our research group have also reported[2,7] that titanium can be used as a doping element into the silicone resin chain through hydrolysis-polycondensation method, leading to an improvement of thermal stability of the silicone resin varnish up to 500°C after doping.

It is well know that boron atom and silicon atom are sharing common characteristics like atomic radius and electronegativity that will facilitate the replacement of silicon atoms by boron atoms in the covalent bonds with oxygen atom. Furthermore, the covalent bond energy of B—O bond is 514 kJ/mol, which is higher than that of Si—O bond (451 kJ/mol). According to this strong bond energy, it may be predicted that some performances would be improved after doping the resin with boron atom. Zhao et al.[8] have prepared boron modified silica coating by sol–gel method with an improvement of hardness and heat resistance of silica coating. Liu et al.[9] also reported the synthesis and the corresponding structural changes of a boron-containing phenol-formaldehyde resin (BPFR) made from boric acid (BA), phenol, and paraformaldehyde. Moreover, some related papers also reported that the element boron can be used as doping agent within siloxane chains and were present in the form of Si—O—B bonds.[9–13] However, there are few reports in the literature related with boron atom doping into silicone resins. In this work, we

Additional Supporting Information may be found in the online version of this article.

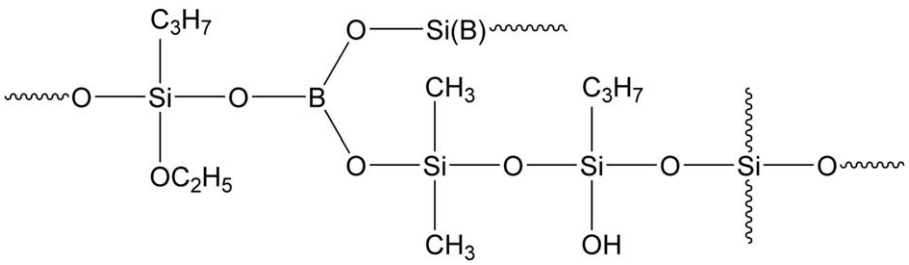

Scheme 1. Chemical structure of boron-doped silicone resin.

describe the use of boron as doping element with the silicone resin molecular chain to improve their thermal stability.

Silicone resins are usually prepared by hydrolysis-polycondensation method with chlorosilane $[(R_1)_nSiCl_{4-n}]$ or alkoxylsilane $[(R_1)_nSi(OR_2)_{4-n}]$ as raw materials. So the properties of silicone resins are closely related to the sort and number of group R_1. To date, most heat-resistant silicone resins contain phenyl groups on the branched-chain because the high phenyl content can increase the thermal stability. However, phenyl chlorosilane or phenyl alkoxylsilane are expensive and poisonous, which results in high costs and pollution. In this study, we used low-cost propyl-triethoxysilane (PTES) and dimethyl-diethoxysilane (DMDES) as raw materials instead of phenyl alkoxylsilane. In addition, we try to make it sure that B—OH from BA can be condensed with Si—OH or Si—OR successively to form cross-linked structure of boron-doped silicone resin (BSR). So the obtained BSR were characterized by Fourier transform infrared spectroscopy (FTIR), X-ray photoelectron spectroscopy (XPS), and nuclear magnetic resonance (NMR). We also discussed the thermal decomposition mechanism and the change of the molecular structure during the degradation process.

EXPERIMENTAL

Materials

Commercial industrial grade PTES and DMDES were purchased from Guangzhou JCZY organic silicone Co. (China) and used as received. Absolute ethyl alcohol (AR), boric acid (AR), and hydrochloric acid were purchased from Guangzhou Huaxin instrument Co. (China) and used without further purification.

Characterization

The FTIR transmission spectra of the samples were recorded from KBr-pellets (1 wt % of polymer) using a Thermo Nicolet 6700 FTIR spectrometer over the range of 4000 to 400 cm^{-1} at 4 cm^{-1} resolution. The NMR analyses were carried out with a Bruker AVANCE Digital 400 MHz spectrometer. The ^{1}H-NMR and ^{11}B-NMR spectra were obtained using deuterated methanol as solvent. XPS spectra were recorded using a ESCALAB 250 (Thermal-VG Scientific) system, Al K_α (1486.6 eV) as X-ray source.

Gel permeation chromatography (GPC) was performed on a Waters 1515 gel permeation chromatograph. The mobile phase was tetrahydrofuran and the flow rate was 1 mL/min at room temperature. The polymer concentration was 10 mg/mL with a 50 μL injection volume.

Thermogravimetric analyses (TGA) and TG-FTIR analyses measurements were conducted using both thermo-gravimetric analyzer(STA 409 PC, NETZSCH) and FTIR spectrometer (Thermo Nicolet 6700) operating at heating rates 10°C/min from 30 up to 800°C under a controlled dry nitrogen flow of 40 mL/min.

Preparation of BSR and PSR

A reaction mixture of 35.0 mL PTES, 6.6 mL dimethyl diethoxy-silane, 20 mL absolute alcohol, and 0.5 mL hydrochloric acid (1 mol/L) were added into a 250 mL four-necked flask equipped with a mechanical stirrer, a water condenser, a thermometer, and with a constant pressure drop funnel. The mixture was vigorously stirred and heated to 65°C, then 4.5 mL deionized water was added dropwise to the stirred mixture within 10 min. After the addition, the reaction mixture was kept isothermally at 65°C and stirred for 2 h. At last, 2.19 g BA as powder was added to the four-necked flask at one-time. The reaction mixture was kept refluxing at 65°C for 1 h, then the hydrolyzate was obtained.

The hydrolyzate was heated to 120°C under vacuum for 30 min to remove the ethanol and other small molecule, a transparent viscous mixture was obtained and recorded as BSR-1#.

A series of BSR with different content of boron were prepared, in which all experimental conditions were the same except for the added quality of BA, and recorded them as BSR-2#, BSR-3#, BSR-4#, BSR-5#, and BSR-6#, respectively.

For comparison, we also prepared pure silicone resin (PSR-1#), in which all experimental conditions were the same with the preparation of BSR except for none of BA added to the reaction mixture.

RESULTS AND DISCUSSION

Synthesis of BSR

In order to obtain the expected products, alkoxy groups Si—OR in PTES and DMDES were hydrolyzed first with H_2O to generate functional groups Si—OH. Subsequently, the condensation reaction between Si—OH and Si—OH or B—OH took place, generating an appropriate degree of cross-linking within silicone resin (Scheme 1). We chose BA (H_3BO_3) as raw material due to the fact that each BA molecule has three hydroxyl groups and its space volume is very small. So the condensation reaction between B—OH and Si—OH or Si—OR took place easily during the preparation step of the BSR. In addition, PTES is tri-functional siloxane and DMDES is di-functional siloxane and

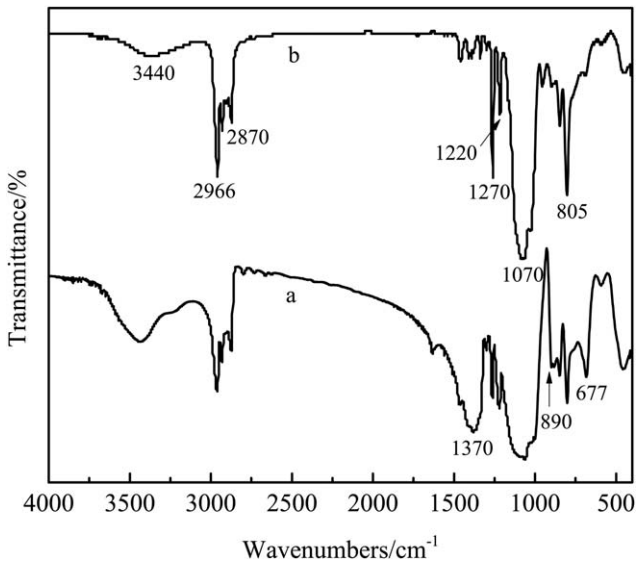

Figure 1. FTIR spectrogram of BSR-1# (curve a) and PSR-1# (curve b).

BA molecules have three reactive groups, it is easy for us to prepare different degrees of cross-linked BSR through adjusting the molar ratio of each reagent.

According to the reaction mechanism described above, it is obvious that such parameter as temperature, catalyst, the ratio of the starting materials influences the structures and properties of the final products. As for the hydrolysis reaction, hydrochloric acid was used as catalyst, the suitable temperature was about 65°C, and the suitable quality of deionized water added to the reaction was just 60% of the calculated amount according to the experimental results. With high temperature and more deionized water, gel produced easily in the reaction system perhaps due to the severe hydrolysis and condensation reaction. In order to obtain a PTES-DMDES-BA copolymer with narrowed molecular weight distributions, the molar ratio of the starting materials and the polycondensation temperature and time were all important. The experimental results demonstrate that the optimum molar ratio of the starting materials PTES/DMDES/BA was in 15 : 4 : 4, and the suitable condensation temperature was 120°C. Based on this study, a novel BSR was prepared successfully and the GPC study demonstrated a single peak with weight-average molecular weight (M_w) of 4044 and molecular weight distribution of 1.21.

Characterization of the BSR

Fourier Transform Infrared Spectroscopy. As shown in Figure 1, curves a and b represent the FTIR spectra of sample BSR-1# and PSR-1#, respectively.

Both spectra exhibited the strong absorption at 3440 cm^{-1}, corresponding to the stretching vibration of ν O—H, the absorption band of 2966 and 2870 cm^{-1} was assigned to the anti-symmetry and symmetry stretching vibration of ν C—H from —CH_3 or —CH_2—CH_2—CH_3.[14,15] The absorption at 1270 cm^{-1} and 1220 cm^{-1} was assigned to the stretching vibration of ν O—C. The strong absorption at 1070 cm^{-1} was assigned to the anti-symmetry stretching vibration of ν Si—O—Si or ν C—C, because the characteristic vibration of them are always overlapping. While the absorption at 805 cm^{-1} was assigned to symmetry stretching vibration of ν Si—O—Si or ν Si—C, which are characteristic for organic silicone resin.

When compared curves a and b, the notable difference between them is the strong absorption peak at 1370 cm^{-1}, which corresponding to stretching vibration of ν B—O. Another difference is that there are two weak absorption peaks at 890 cm^{-1} and 677cm^{-1} in curve a, which corresponds to stretching vibration of ν B—O—Si and in-plane shear vibration of δ B—O—Si, respectively.[9,11,16] These results suggest that boron atom has been successfully doped into the silicone resin chain in the form of Si—O—B bond by the method of hydrolysis-polycondensation.[7,17–19]

Nuclear Magnetic Resonance. The ^{1}H-NMR spectrogram of PTES, DMDES, and product BSR-1# is shown in Figure 2. In Figure 2(a), peaks at δ 0.53–0.57, 1.34–1.40, and 0.91–0.95 correspond to Si—CH_2— (a), —CH_2— (b), and CH_3— (c) hydrogen of propyl group on PTES,[20] respectively. In addition, the δ 3.71–3.76 and 1.12–1.16 hydrogen peaks belong to the —CH_2— (d) and CH_3— (e) of the ethoxy groups on PTES, respectively. In Figure 2(b), peak at δ 0.41 corresponds to Si—CH_3 (a) on the DMDES, hydrogen peaks at δ 3.65–3.71 and 1.11–1.15 correspond to CH_3—CH_2O (b) and CH_3— (c) of the ethoxy groups on the DMDES respectively,[20] which is similar to PTES.

In the spectrogram of product BSR-1#, peak at δ 4.84 corresponds to hydroxyl group Si—OH (a) obtained from hydrolysis of the starting materials. The hydrogen peaks δ 0.10–0.15 belong to the methyl groups on DMDES block,[20] which is linked directly to the Si atom Si—CH_3 (b). Peaks at δ 0.63, 1.49, and 0.99 correspond to Si—CH_2— (c), —CH_2— (d), and CH_3— (e) hydrogen peaks of propyl group on PTES block. In addition, peaks at δ 3.58–3.64 and 1.16–1.21 perhaps belong to —CH_2— (f) and CH_3— (g), respectively, the ethoxy groups that did not take part in the hydrolysis. The analyses of the ^{1}H-NMR spectra demonstrate that most starting materials PTES and DMDES were co-condensed successfully after the hydrolysis reaction.

The ^{11}B-NMR spectrogram is shown in Figure 3. The boron peak at δ 19.70 ppm corresponds to B—OH, which is characteristic for BA (H_3BO_3).[21] There is only one strong single peak at δ 18.55 ppm for the product BSR, and it shifted to low field compared with the BA, suggesting that boron atom in BSR only in a chemical state which is different with BA and boron atom doped into silicone resins successfully.

X-ray Photoelectron Spectroscopy. XPS measurements provide further evidence for the reaction of BA with the two siloxane monomers. Figure 4 displays the wide scanning spectra of XPS of sample BSR-1#. The binding energy at 532.28 eV is attributed to O1s, the binding energy at 284.78 eV belongs to C1s, whereas peak at 184.47 eV and 102.34 eV correspond to Si2s and Si2p, respectively.[22] Because the intensity of the binding energy with peak at 193.33 eV which belongs to B1s, is not so strong, the narrow scanning spectra of B1s was performed and showed in Supporting Information. Both of them demonstrated that the

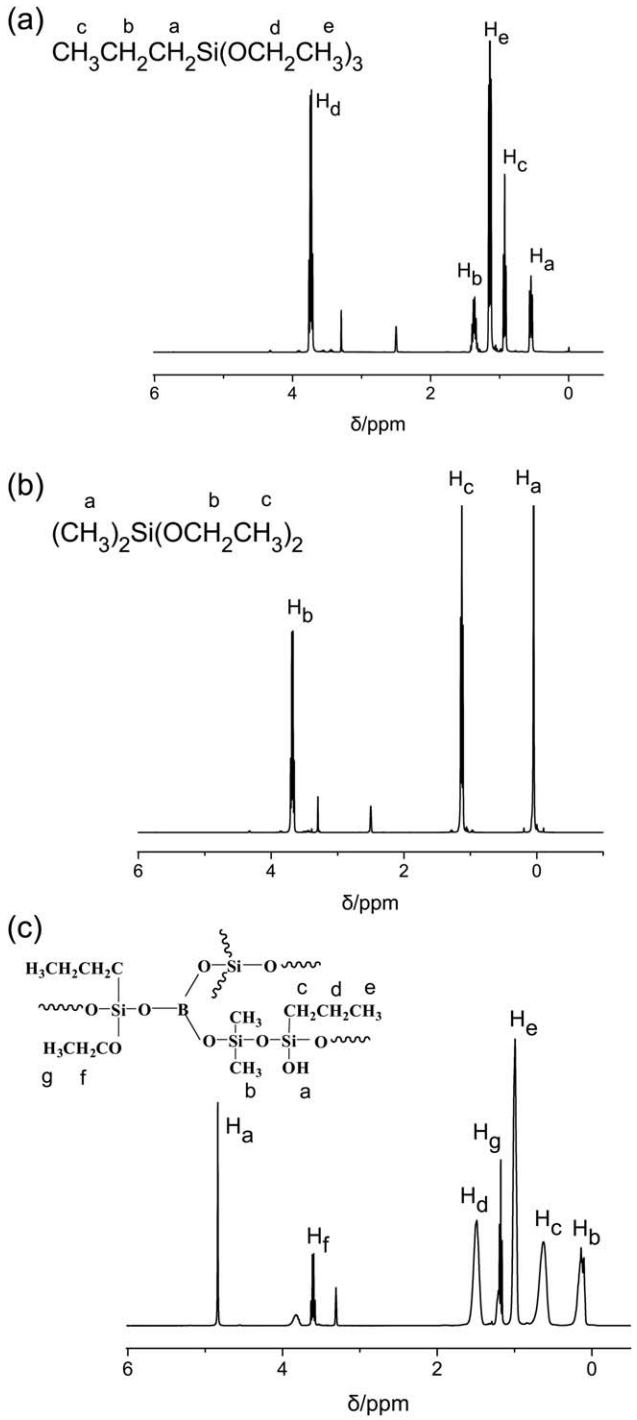

Figure 2. [1]H-NMR spectrogram of PTES (a), DMDES (b), and BSR-1# (c): (a) PTES, (b) DMDES, and (c) BSR-1#.

element boron was detected in the XPS spectra, and the boron element of the XPS curve was Gaussian distribution, suggesting that the boron atoms only in a chemical state in BSR. The binding energy at 193.33 eV is consistent with bond B—O,[23] means that the boron atoms exist in the main chain of BSR as Si—O—B motifs.

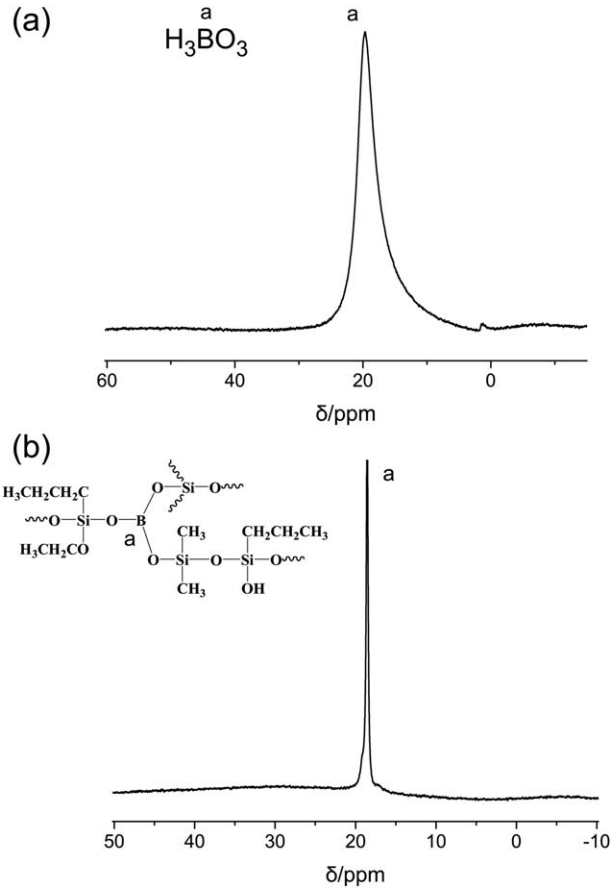

Figure 3. [11]B-NMR spectrogram of H_3BO_3 (a) and BSR-1# (b): (a) H_3BO_3 and (b) BSR-1#.

The narrow scanning spectra of C1s XPS of sample BSR-1# were also presented in Supporting Information. Table I shows the results of the analyses of the peaks of the C1s XPS spectra. The asymmetrical C1s XPS suggest that the carbon atoms in BSR are in different chemical states. The binding energy at 284.10 eV is attributed to C atoms of methyl groups bonded to Si atom, whereas the binding energy with peak at 284.47 eV corresponds to C atoms of propyl groups bonded to Si atom. The binding energy of the dominating component at 285.01 eV can be attributed to the C—C bonds[24,25] and the smallest area of the peak at 285.89 eV to the C atoms of O—C_2H_5 of incompletely hydrolyzed Si—OC_2H_5 groups.[25,26] According to Table I, the relative proportion of different chemical states of C atoms is consistent with the proposed structures of the modified resin.

According to the above analysis, PTES DMDES, and BA all participated in the polycondensation reaction for preparing BSR. The result was consistent well with that obtained by infrared characterization and NMR analysis.

Thermal Stability Properties. Figure 5 shows the TGA (a) and derivative thermogravimetry (DTG) (b) thermogram of the viscous resin sample of PSR-1# and BSR-1#, respectively. It can be seen that the thermal degradation of PSR and BSR appear as a multistage reaction. According to these curves, the degradation

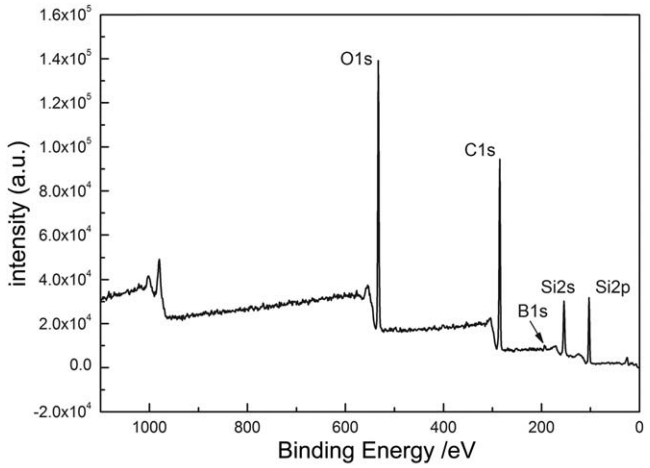

Figure 4. Wide scanning spectra of XPS of BSR-1#.

process can be divided into two stages. As for PSR, the weight loss in the first stage between 160 and 320°C is about 65%, whereas the weight loss in the second stage between 500 and 560°C is about 10%, leaving a stabilized residue of ~25.5% when the temperature is higher than 600°C. According to the residue weight percentage, we predicted the residue was silicon oxide, which agreed well with the theoretical value 26.1%.

Similar weight loss stages could be observed for the BSR-1#. Notably, there is almost no weight loss from room temperature to 400°C. The main weight loss was from 400°C to 500°C, followed by a further slight weight loss between 500 and 560°C, leaving a stabilized residue of 50.5% when the temperature is higher than 600°C. For BSR, the residue may be a mixture of silicon oxide and boron oxide.[27]

According to the results of TGA and DTG, we conclude that the thermal stability of the boron-doped silicon resin has been greatly improved compared to the normal silicone resin. Such stability improvement might be explained by the formation of the Si—O—B bond network that protects the small groups of the side-chains from a thermal decomposition.[27–30] In addition, compared with Si—O bond, the high bond energy of B—O bond (514 kJ/mol) also contributes to the improvement of the thermal stability of resin.

To study the thermal stability of BSR more comprehensively, a series of samples doped with different degree of boron were examined by TGA. Degradation temperatures at 5, 10, and 50% weight loss of composites and the char residue at 800°C are given in Table II, $T_{5\%}$, $T_{10\%}$, and $T_{50\%}$ are temperatures corresponding to 5, 10, and 50% weight loss, respectively, which are the main criteria indicating the thermal stability of the composites, the higher is the values, the higher is the thermal stability.[27]

$T_{5\%}$, $T_{10\%}$, and $T_{50\%}$ data indicate an increasing thermal stability of BSR with different degree of boron compared with PSR. The thermal stability of BSR is influenced by the boron content. When compared with the data of the first 3 groups in Table II, it shows increasing the content of boron causes the decline of thermal stability of BSR. When compared with the data of the last three groups, the results are just opposite, that increasing the content of boron causes the increase of thermal stability of BSR. Therefore, the sample BSR-1# with optimum boron content demonstrates the best thermal stability, there is almost no weight loss from room temperature to 400°C. The results might be explained by the direct relationship of structure and thermal stability. Because the reactivity of three raw materials are different, it is very important to control the ratio of the reactants to make sure polycondensation evenly, which results in homogeneous distribution of boron on silicone resins network to form strong Si—O—B bond and excellent thermal resistance. When

Table I. Peak Analysis Results of the C1s XPS Spectra

Peak position	284.10 eV	284.47 eV	285.01 eV	285.89 eV
Corresponding atom	C—Si	C—C—C*—Si	C—C	C—O
% of total area	16.5	23.6	54.4	5.5

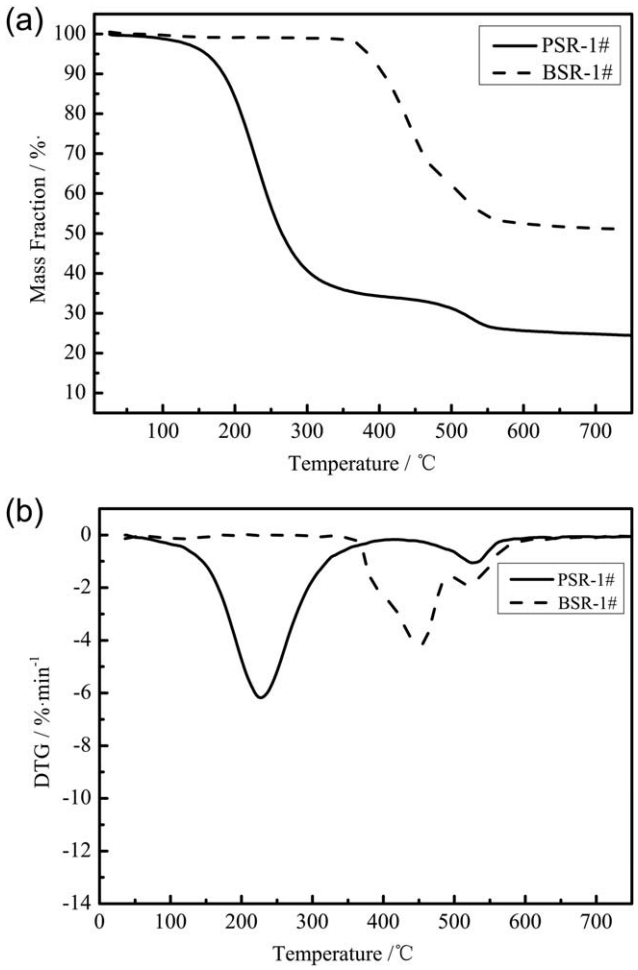

Figure 5. TGA (a) and DTG (b) curves for PSR-1# and BSR-1#: (a) TGA and (b) DTG. [Color figure can be viewed in the online issue, which is available at wileyonlinelibrary.com.]

Table II. Thermal Properties of PSR and BSR

Sample	n_{B-OH}/n_{Si-OR}*	$T_{5\%}$ (°C)	$T_{10\%}$ (°C)	$T_{50\%}$ (°C)	Char residue (%)
BSR-1#	1 : 5	405	411	-	50.5
BSR-2#	1 : 4	340	364	450	34.5
BSR-3#	1 : 3	316	348	431	32.0
BSR-4#	1 : 8	216	326	-	55.0
BSR-5#	1 : 7	217	319	430	35.0
BSR-6#	1 : 6	238	321	421	31.0
PSR	-	162	185	266	25.5

n_{B-OH}/n_{Si-OR}* means the molar ratio of B—OH in boric acid and Si—OR in PTES-DMDES.

doped with the more or less content of boron, it is difficult for boron to be distributed evenly on the resins network and causes the decline of thermal stability.

The char residue data given in Table II were obtained after the weight of the samples remain constant when the heated temperature up to 800°C. It indicates there is more residue of BSR with different degree of boron compared with PSR. The amount of the residue of BSR is not connected with and proportional to the boron content directly. According to the residue weight, the main remained composites are SiO_2 and/or B_2O_3.[27]

Thermal Degradation Mechanism. To study the thermal degradation mechanism of BSR, the sample BSR-1# was heated in the muffle furnace at heating rates 4°C/min from room temperature to 350, 400, or 600°C, respectively. FTIR spectra of the residue at different temperature were showed in Figure 6. Also, TGA-FTIR analysis measurements were conducted, operating at heating rates 10°C/min from room temperature to 800°C under a controlled dry nitrogen flow of 40 mL/min. FTIR spectra of the cracked gases at different temperature were showed in Figure 7, curves a, b, c, d, and e present the FTIR spectra at different time and different temperature, respectively.

In Figure 6, when compared with curve a, the curve b was mainly unchanged, suggesting that the groups both on the side chains and on the main chains were intact, which agrees well with the TGA-FTIR measurements in Figure 7 curve a, there is almost no signals detected after heated for 32 min and the temperature up to 350°C. Both results mean that the thermal stability of the BSR improved greatly compared with PSR. However, with rising temperature beyond 400°C, the absorptions of C—H at 2965–2870 cm^{-1} decrease first, then the absorptions of O—H and C—O groups at 3440, 1270 cm^{-1}, 1220 cm^{-1} in Figure 6 decrease rapidly. After 420°C, the absorptions of C—H almost disappear. These IR absorption variations indicate that, the BSR degradation begins with the breaking small groups as —CH_3 and —C_3H_7 from the side chains. This process is confirmed by the increased absorption bands at 2966 cm^{-1}, 2880 cm^{-1}, 1270 cm^{-1}, 1220 cm^{-1}, and1115 cm^{-1} in Figure 7 (curve c, when the sample heated for 40 min and temperature up to 430°C), which may be assigned to the stretching vibration of *v*

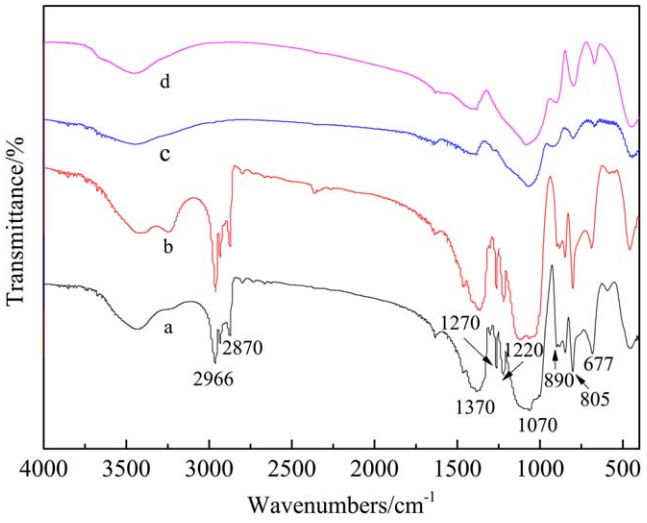

Figure 6. FTIR spectra of the residue of boron-doped silicone resin heated at different temperature: curve a, room temperature; curve b, 350°C; curve c, 400°C; curve d, 600°C. [Color figure can be viewed in the online issue, which is available at wileyonlinelibrary.com.]

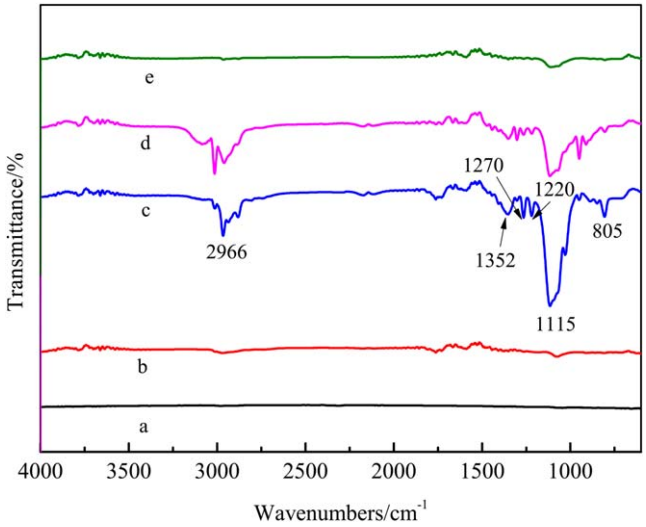

Figure 7. FTIR spectra of the cracked gas from BSR at different time and different temperature; curve a: $t = 0$ min, $T = 30$°C (room temperature); curve b: $t = 32$ min, $T = 350$°C; curve c: $t = 40$ min, $T = 430$°C; curve d: $t = 50$ min, $T = 530$°C; curve e: $t = 60$ min, $T = 630$°C. [Color figure can be viewed in the online issue, which is available at wileyonlinelibrary.com.]

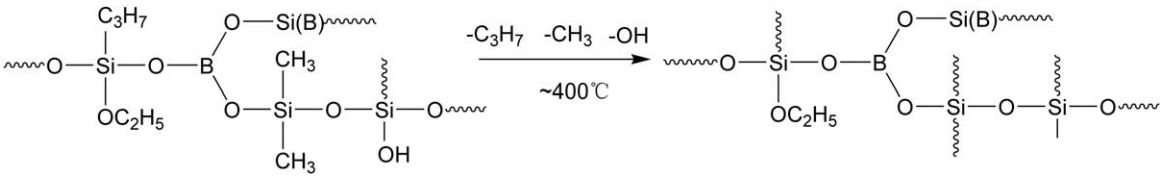

Scheme 2. The first stage of BSR thermal degradation.

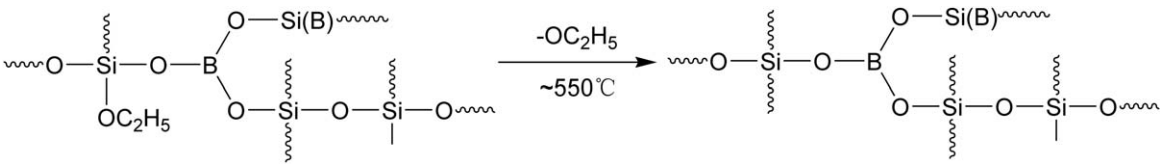

Scheme 3. The second stage of BSR thermal degradation.

C—H, and the stretching vibration of *v* C—O or *v* C—C, respectively.[14,15] With the increase of temperature, the intensity of these absorption bands increased gradually.

When comparing curves c and d in Figure 6, the spectra are mainly unchanged except the small band at 1270 cm^{-1}, which is due to O—C_2H_5 on the Si—OC_2H_5 groups that disappeared at 600°C. The small absorption peak at 1270 cm^{-1} and the small weight loss of the DTG spectra at 520°C are consistent with the small amount of Si—OC_2H_5 groups present in the silicone resin,[31] which is demonstrated from the analyses of C1s XPS of sample BSR-1#, the smallest area (5.5% of total area) of the peak at 285.89 eV corresponding to C atoms from Si—OC_2H_5 groups owing to incompletely hydrolyzed. In the other hand, the relative high binding energy in XPS of this kind of C atoms (Si—OC_2H_5) also indicates that the connection of O—C in this groups are more stable, which is consistent with the relative high temperature for the second degradation stage in DTG thermogram in Figure 5. However, there is no significant difference in Figure 7 (curve c and d) except for the intensity of absorption bands when heated from 430°C to 530°C, this may be caused by the similar characteristic stretching vibration of O—C_2H_5 with —CH_3, —C_3H_7, and C—O groups.

The above analytical data described suggest a two-stage thermal degradation process for BSR. The first stage is cleavage of a majority of small groups including —CH_3, —C_2H_5, and —OH groups from the side chains, as represented in Scheme 2. The second stage is the cleavage of the residual small amounts of Si—OC_2H_5 groups at higher temperature, as depicted in Scheme 3. Throughout the thermal degradation, Si—O—Si bonds and Si—O—B bonds of the main chains remained intact, which is certified with the characteristic absorption peak at 1370 cm^{-1} (*v* B—O), 1070 cm^{-1} (v_{as} Si—O—Si), 805 cm^{-1} (v_s Si—O—Si), and 677 cm^{-1} (*v* Si—O—B) in Figure 6 (curves c and d). There is almost no signals detected after heated for 60 min and the temperature up to 630°C in Figure 7 (curve e) also indicated that the degradation finished and the residue was stable.

CONCLUSIONS

In this manuscript, we report the preparation of a novel BSR synthesized from BA, PTES, and DMDES by hydrolysis-polycondensation method. Both NMR spectra and XPS analyses confirmed that elemental boron has been introduced as doping agent within the main chains of the silicone resin as Si—O—B bond motifs.

The thermal properties of these resins have also been investigated and the results clearly indicated that the boron doping largely improved the thermal stability of silicone resins and the thermal stability of the BSR was influenced by the content of boron. The thermal degradation of BSR occurred into two stages: the first stage was the loss of substituent such as methyl and propyl, the second stage was the cleavage of small amounts of alkoxy groups.

ACKNOWLEDGMENTS

The authors thank the Science and Technology Project of Guangdong Province (Project No. 2012B010200034) for financial support. Zhi-Feng Hao is thankful to Prof. Bernard Meunier for the modification and guidance of this manuscript.

REFERENCES

1. Hajji, P.; David, L.; Gerard, J. F.; Pascault, J. P. Vigier, G. *J. Polym. Sci. Part B: Polym. Phys.* **1999**, *37*, 3172.
2. Wang, X. M.; Wu, Y. H.; Hao, Z. F.; Yu, J.; Yu, L. *Chem. Res. Chin. Univ.* **2010**, *26*, 851.
3. Wei, Y.; Jin, D. L.; Xu, J. G.; Baran, G.; Qiu, K. Y. *Polym. Adv. Technol.* **2011**, *12*, 361.
4. Wu, K. H.; Chang, T. C.; Wang, Y. T.; Chiu, Y. S. *J. Polym. Sci. Part A: Polym. Chem.* **1999**, *37*, 2275.
5. Zhu, Z. K.; Yang, Y.; Yin, J.; Qi, Z. N. *J. Appl. Polym. Sci.* **1999**, *73*, 2977.
6. Zhang, A. L.; Liu, H.; Wu, S. H. In International Conference on Electronics, Communications and Control (ICECC), Ningbo, China, **2011**; p 3888–3891.
7. Wang, X. M.; Hao, Z. F.; Liao, X. Q.; Tang, B. Z.; Yu, J.; Yu, L. *Paint Coat. Ind.* **2010**, *40*, 5.
8. Zhao, X.; He, X. D.; Zhang, S.; Wang, L. D.; Li, M. W.; Li, Y. B. *Thin Solid Films* **2011**, *519*, 4849.

9. Liu, Y. F.; Gao, J. G.; Zhang, R. Z. *Polym. Degrad. Stab.* **2002**, *77*, 495.
10. Barros, P. M.; Yoshida, I. V. P.; Schiavon, M. A. *J. Non-Cryst. Solids* **2006**, *352*, 3444.
11. Mondal, S.; Banthia, A. K. *J. Eur. Ceram. Soc.* **2005**, *25*, 287.
12. Hasegawa, I.; Fujii, Y.; Takayama, T.; Yamada, K. *J. Mater. Sci. Lett.* **1999**, *18*, 1629.
13. Sinha, A.; Mahata, T.; Sharma, B. P. *J. Nucl. Mater.* **2002**, *301*, 165.
14. Gervais, C.; Babonnrau, F.; Dallabonna, N.; Soraru, G. D. *J. Am. Ceram. Soc.* **2001**, *84*, 2160.
15. Guo, F.; Xia, X. N.; Xiong, Y. Q.; Liu, J.; Xu, W. J. *J. Appl. Polym. Sci.* **2012**, *125*, 104.
16. Shen, J.; Jiang, W.; Liu, Y.; Wei, R. Q.; Liu, X. N.; Zhong, Y.; Xu, J.; Li, L. L.; Xue, G. *J. Appl. Polym. Sci.* **2012**, *24*, 3905.
17. Nogami, M.; Moriya, Y. *J. Non-Cryst. Solids* **1982**, *48*, 359.
18. Liu, Y.; Yan, G. P.; Che, H. W.; Wang, X. Y.; Guo, Q. Z. *J. Appl. Polym. Sci.* **2011**, *119*, 1156.
19. Gao, J. G.; Jiang, C. J.; Ma, W. T. *Polym. Compos.* **2008**, *29*, 274.
20. Tonelli, A. E. NMR Spectroscopy and Polymer Microstructure; VCH: New York, **1989**.
21. Li, J.; Li, W.; Gao, S. Y. *J. Salt Lake Sci.* **1995**, *3*, 72.
22. Briggs, D. Surface Analysis of XPS and Static SSIMS; Cambridge University Press: Cambridge, United Kingdom, **2001**.
23. Soraru, G. D.; Dallabona, N.; Gervais, C.; Babonneau, F. *Chem. Mater.* **1999**, *11*, 910.
24. Zhou, Z. F.; Bello, I.; Lei, M. K.; Li, K. Y.; Lee, C. S.; Lee, S. T. *Surf. Coat. Technol.* **2000**, *128*, 334.
25. Liu, Y. H.; Jiang, X. L. *Carbon* **2007**, *45*, 1965.
26. Chen, C. H.; Yen, W. S.; Kuan, H. C.; Kuan, C. F.; Chiang, C. L. *Polym. Compos.* **2010**, *31*, 18.
27. Ahmetli, G.; Deveci, H.; Soydal, U.; Gurler, S. P.; Altun, A. *J. Appl. Polym. Sci.* **2012**, *125*, 38.
28. Pandey, P.; Anbudayanidhi, S.; Mohanty, S.; Nayak, S. K. *Polym. Compos.* **2012**, *33*, 2058.
29. Darras, V.; Fichet, O.; Perrot, F.; Boileau, S.; Teyssie, D. *Polymer* **2007**, *48*, 687.
30. Balizer, E.; Duffy, J. D. *Polymer* **1992**, *33*, 2114.
31. Kirubaharan, A. M. K.; Palraj, S.; Selvaraj, M.; Rajagopal, G. *J. Appl. Polym. Sci.* **2011**, *119*, 2339.